Hypernetwork-Based Augmentation

Chih-Yang Chen¹, Che-Han Chang¹, and Edward Y. Chang^{1,2}

¹HTC Research & Healthcare

²Stanford University

{harry.cy_chen,chehan_chang,edward_chang}@htc.com

Abstract

Data augmentation is an effective technique to improve the generalization of deep neural networks. Recently, AutoAugment [1] proposed a well-designed search space and a search algorithm that automatically finds augmentation policies in a data-driven manner. However, AutoAugment is computationally intensive. In this paper, we propose an efficient gradient-based search algorithm, called Hypernetwork-Based Augmentation (HBA), which simultaneously learns model parameters and augmentation hyperparameters in a single training. Our HBA uses a hypernetwork to approximate a population-based training algorithm, which enables us to tune augmentation hyperparameters by gradient descent. Besides, we introduce a weight sharing strategy that simplifies our hypernetwork architecture and speeds up our search algorithm. We conduct experiments on CIFAR-10, CIFAR-100, SVHN, and ImageNet. Our results demonstrate that HBA is significantly faster than state-of-the-art methods while achieving competitive accuracy.

1 Introduction

Data augmentation techniques, such as cropping, horizontal flipping, and color jittering, are widely used in training deep neural networks for image classification. Data augmentation acts as a regularizer that reduces overfitting by transforming images to increase the quantity and diversity of training data. Recently, data augmentation has shown to be an effective technique not only for supervised learning [1, 2, 3], but also for semi-supervised learning [4, 5], self-supervised learning [6], and reinforcement learning (RL) [7]. However, given a new task or dataset, it is non-trivial to either manually or automatically design its data augmentation policy: determine a set of augmentation functions and adequately specify their configurations, such as the range of rotation, the size of cropping, the degree of color jittering. A weak augmentation policy may not help much, while a strong one could hinder performance by making an augmented image looks inconsistent to its label.

AutoAugment [1], a representative pioneering work proposed by Cubuk et al., proposed a search space (consisting of 16 image operations) and an RL-based search algorithm to automate the process of finding an effective augmentation policy over the search space. AutoAugment made remarkable improvements in image classification. However, its search algorithm requires 5000 GPU hours for one augmentation policy learning, which is extremely computationally intensive.

To address the computational issue, we formulate the augmentation policy search problem as a hyperparameter optimization problem and propose an efficient algorithm for tuning data augmentation hyperparameters. The central idea of our method is a novel combination of a population-based training algorithm and a *hypernetwork*, which is a function that outputs the weights of a neural network. In particular, we introduce a population-based training procedure and four modifications to derive our algorithm. First, we employ a hypernetwork to represent the set of models. By doing so, training a hypernetwork can be treated as training a *continuous* set of models. Second, instead of evaluating the performance on a discrete set of models, thanks to the use of a hypernetwork, we can perform gradient descent and back-propagate gradients through the hypernetwork to efficiently find the approximate best model from the continuous set of models. Third, we propose a new hyper-layer for batch normalization [8] to facilitate the construction of hypernetworks. The resulting algorithm resembles the recently proposed Self-Tuning Network (STN) algorithm [9] but is derived entirely

Table 1: Our HBA is at least an order of magnitude faster than AutoAugment (AA), Population Based Augmentation (PBA), and Fast AutoAugment (FAA), while achieving similar accuracy.

Dataset	Model		AA [1]	PBA [2]	FAA [3]	HBA
CIFAR-10 [13]	Wide-ResNet-28-10 [14]	GPU Hours Test Error (%)	5000 2.6	5 2.6	3.5 2.7	0.1 2.6
SVHN [15]	Wide-ResNet-28-10 [14]	GPU Hours Test Error (%)	1000 1.1	1 1.2	1.5 1.1	0.1 1.1
ImageNet [16]	ResNet-50 [17]	GPU Hours Test Error (%)	$15000 \\ 22.4$	-	450 22.4	0.9 22.1

from a different perspective. Fourth, inspired by one-shot neural architecture search [10, 11, 12], we adopt a weight sharing strategy to the models. We show that such a strategy corresponds to a simplified hypernetwork architecture that effectively reduces the search time and slightly improves the accuracy. Our method, dubbed as Hypernetwork-Based Augmentation (HBA), is a *gradient-based* method that jointly trains the network model and tunes the augmentation hyperparameters. HBA yields hyperparameter schedules that can be used to train on different datasets or to train different network architectures. Experimental results show that HBA achieves significantly faster search speed while maintaining competitive accuracy. Table 1 summarizes our main results.

Our contributions can be summarized as follows. (1) We propose Hypernetwork-Based Augmentation (HBA), an efficient gradient-based method for automated data augmentation. (2) The derivation of our HBA algorithm reveals the underlying relationship between population-based and gradient-based methods. (3) We propose a weight-sharing strategy that simplifies our hypernetwork architecture and reduces the search time considerably.

2 Related work

Data Augmentation. We review previous work relevant to the development of our method. We refer readers to a comprehensive survey paper [18] on data augmentation. Hand-designed data augmentation techniques, such as horizontal flipping, random cropping, and color transformations, are commonly used in training deep neural networks for image classification [19, 17]. In recent years, several effective data augmentation techniques are proposed. Cutout [20] randomly erases contents by sampling a patch from the input image and replace it with a constant value. Mixup [21] performs data interpolation that combines pairs of images and their labels in a convex manner to generate virtual training data. CutMix [22] generates new samples by cutting and pasting image patches within mini-batches. These data augmentation techniques are hand-designed, and their hyperparameters are usually manually-tuned.

Automated Data Augmentation. Inspired by recent advances in neural architecture search [23, 10, 24], one of the recent trends in data augmentation is automatically finding augmentation policies within a pre-defined search space in a data-driven manner. AutoAugment [1] introduced a well-designed search space and proposed an RL-based search algorithm that trains a recurrent neural network (RNN) controller to search effective augmentation policies within the search space. Although AutoAugment achieves promising results, its search process is computationally expensive (5000 GPU hours on CIFAR-10). Our algorithm treats the data augmentation hyperparameters as continuous variables, and efficiently optimizes them by gradient descent in a single round of training.

Recently, several efficient search algorithms based on AutoAugment's search space have been proposed. Population Based Augmentation (PBA) [2] employed Population Based Training (PBT) [25], an evolution-based hyperparameter optimization algorithm, to search data augmentation schedules. Fast AutoAugment [3] treats the problem as a density matching problem and used Bayesian optimization to find augmentation policies. OHL-Auto-Aug [26] proposed an online hyperparameter learning algorithm that jointly learns network parameters and augmentation policy. Our algorithm also tunes augmentation hyperparameters in an online manner while achieves better search efficiency. RandAugment [27] simplified the search space of AutoAugment and used the grid search method to find the optimal augmentation policy. Differentiable Automatic Data Augmentation (DADA) [28], inspired by Differentiable Architecture Search (DARTS) [24], proposed a gradient-based method that relaxes the discrete policy selection to be differentiable and optimize the augmentation policy by stochastic gradient descent. Our algorithm is also gradient-based but is fundamentally different from

DADA. DADA is based on differentiable relaxation, while ours is based on population-based training and hypernetworks.

Hypernetworks. Ha et al. [29] used hypernetworks to generate weights for recurrent networks. SMASH [11] presented a neural architecture search method that employs a hypernetwork to learn a mapping from a binary-encoded architecture space to the weight space. Self-Tuning Network (STN) [9] used a hypernetwork as an approximation to the best response function in bilevel optimization. Our method uses a hypernetwork to represent a set of models trained with different hyperparameters.

Hyperparameter Optimization. Searching data augmentation policies can be formulated as a hyperparameter optimization problem. We refer readers to a recent survey paper [30] on hyperparameter optimization. Population Based Training (PBT) [2] presented a generic hyperparameter optimization algorithm that trains a population of models in parallel, and periodically evaluates their performance to perform the so-called "exploit-and-explore" procedure. Recently, MacKay et al. proposed the Self-Tuning Network (STN) [9], a gradient-based method for tuning regularization hyperparameters, including data augmentation and dropout [31]. Our work is closely related to PBT [25] and STN [9]. In our method, we start from a population-based training algorithm and apply a series of modifications to reach our algorithm, which resembles the STN algorithm. Our algorithm can be viewed as an efficient approximation of the PBT algorithm. Compared with STN, our work distinguishes from STN in three aspects. First, STN is based on the best response approximation to bilevel optimization, while our HBA is derived entirely from the perspective of population-based training. Thus, our method can be viewed as a new and novel interpretation of STN. Second, to facilitate the construction of hypernetworks, we propose a new hyper-layer for batch normalization. Third, our method employs a weight sharing strategy to improve both the accuracy and search time.

3 Method

Our proposed method HBA consists of two components: a search space and a search algorithm. We describe our search space in Section 3.1 and our search algorithm in Section 3.2, 3.3, and 3.4. We start from a baseline algorithm (Section 3.2) and then present a series of modifications to derive HBA (Section 3.3 and 3.4). Finally, we present our hypernetwork architecture and the proposed weight sharing strategy in Section 3.5.

3.1 Search Space

We define a data augmentation policy as a stochastic transformation function constructed by a set of elementary image operations. Each operation is associated with a probability and a magnitude, which play the role of data augmentation hyperparameters. For a fair comparison in the experiments, our transformation function follows PBA [2], which consists of 15 operations and performs three steps: (1) sampling an integer $K \in \{0,1,2\}$ from a categorical distribution as the number of operations to be applied, (2) sampling K out of the 15 operations based on the operation probabilities, and (3) sequentially applying these sampled operations to the input image. Please refer to Appendix A and PBA [2] for the details of the PBA search space. We note that unlike PBA, which discretizes continuous hyperparameters, we treat all hyperparameters as continuous variables.

3.2 Training a Population of Models by Stochastic Gradient Descent

We formulate tuning data augmentation hyperparameters as training a population of n models. Each model i starts from a different initialization of both model parameters θ_i and hyperparameters λ_i . During training, we periodically *exploit* the best performing model and *explore* its hyperparameters and parameters. Specifically, our baseline algorithm is defined as a population-based training procedure that iterates the following three steps.

Update. For each model i, we update its parameters θ_i by T_{train} steps of stochastic gradient descent (SGD) with a learning rate of α and a batch size of 1, which can be expressed as

$$\theta_i = \theta_i - \alpha \nabla_{\theta} \mathcal{L}(\mathcal{F}(\mathcal{A}(x; \lambda_i); \theta_i), y), \tag{1}$$

where (x, y) is the training example, $\mathcal{F}(; \theta_i)$ is the *i*-th model, $\mathcal{A}(; \lambda_i)$ is the augmentation policy used for model i, and \mathcal{L} is the loss function.

Evaluate. We evaluate each model i on the validation set D_V and identify the best performing model k where $k = \arg\min_{i \in \{1, ..., n\}} \sum_{(x^v, y^v) \in D_V} \mathcal{L}(\mathcal{F}(x^v; \theta_i), y^v)$.

Exploit-and-Explore. As exploitation, we select the best performing model k and copy its parameters and hyperparameters to replace the ones of all the other models. Then, for each model, we perform

exploration by perturbing the value of its parameters and hyperparameters with Gaussian noise. This step can be expressed as $\lambda_i = \lambda_k + \epsilon_i$ and $\theta_i = \theta_k + \epsilon_i'$, where $\epsilon_i \sim N(0, \sigma)$ and $\epsilon_i' \sim N(0, \sigma')$ are Gaussian noise. Algorithm 1 shows the baseline algorithm described above. In terms of the exploitation-exploration tradeoff, we can see that our baseline algorithm emphasizes on exploitation.

Algorithm 1 The baseline algorithm of HBA.

```
1: Input: population size n, number of steps T_{outer} and T_{train}, training set D_T, augmentation
      policy A, neural network F, learning rate \alpha, validation set D_V, Gaussian sigma \sigma and \sigma'.
     Initialize \{\theta_i\}_{i=1}^n and \{\lambda_i\}_{i=1}^n
 3: for j = 1 to T_{outer} do
 4:
          for i = 1 to n (synchronously in parallel) do
 5:
              for t=1 to T_{train} do
 6:
                  Sample (x, y) from D_T
                  \theta_i = \theta_i - \alpha \nabla_{\theta} \mathcal{L}(\mathcal{F}(\mathcal{A}(x; \lambda_i); \theta_i), y)
 7:
              end for
 8:
 9:
          k = \arg\min_{i \in \{1,\dots,n\}} \sum_{(x^v,y^v) \in D_V} \mathcal{L}(\mathcal{F}(x^v;\theta_i), y^v)
10:
          for i = 1 to n do
11:
              \begin{array}{l} \lambda_i = \lambda_k + \epsilon_i \text{ where } \epsilon_i \sim N(0,\sigma) \\ \theta_i = \theta_k + \epsilon_i' \text{ where } \epsilon_i' \sim N(0,\sigma') \end{array}
12:
13:
14:
15: end for
16: Output: \theta_k
```

3.3 Representing a Population of Models by a Hypernetwork

We define a hypernetwork as a neural network $\hat{\theta}_{\phi}$ that takes the data augmentation hyperparameters λ as inputs and outputs the parameters θ of the neural network \mathcal{F} . ϕ is the parameters of the hypernetwork to be learned. We use a hypernetwork $\hat{\theta}_{\phi}$ to represent the members of the population by $\theta_i = \hat{\theta}_{\phi}(\lambda_i)$ for $i \in \{1, ..., n\}$. With $\hat{\theta}_{\phi}$, the three steps of the training procedure are modified as follows.

Update. Training a population of models with parameters $\{\theta_i\}_{i=1}^n$ is changed into training a single hypernetwork with parameters ϕ . The SGD update formula in Equation 1 is accordingly changed as

$$\phi = \phi - \alpha \frac{1}{n} \sum_{i=1}^{n} \nabla_{\phi} \mathcal{L}(\mathcal{F}(\mathcal{A}(x_i; \lambda_i), \hat{\theta}_{\phi}(\lambda_i)), y_i).$$
 (2)

Comparing with Equation 1 that independently updates θ_i by SGD with a batch size of 1, Equation 2 updates ϕ by SGD with a batch size of n.

Evaluate. This step is expressed as
$$k = \arg\min_{i \in \{1,...,n\}} \sum_{(x^v,y^v) \in D_V} \mathcal{L}(\mathcal{F}(x^v; \hat{\theta}_{\phi}(\lambda_i)), y^v).$$

Exploit-and-Explore. This step is simplified into $\lambda_i = \lambda_k + \epsilon_i$. θ_i disappears and is implicitly expressed by $\hat{\theta}_{\phi}(\lambda_k + \epsilon_i)$, which can be seen as an approximation of $\hat{\theta}_{\phi}(\lambda_k) + \epsilon_i'$. Up to now, we have used a hypernetwork to reformulate a population-based training as a single hypernetwork training, which we show in Algorithm 4 in Appendix B. We continue deriving our algorithm and then detail the design and construction of our hypernetwork architecture in Section 3.5.

3.4 Approximating Model Selection by Stochastic Gradient Descent

A hypernetwork, as a continuous function, represents a continuous set of models. Therefore, instead of finding the best performing model within the set of n models, which is computationally heavy, we propose to solve $\min_{\lambda} \sum_{(x^v,y^v) \in D_V} \mathcal{L}(\mathcal{F}(x^v;\hat{\theta}_{\phi}(\lambda),y^v))$ approximately by SGD. The Evaluate step is modified as follows.

Evaluate. Given the current hyperparameters λ , we apply T_{val} steps of SGD on the validation set as

$$\lambda = \lambda - \alpha' \frac{1}{n} \sum_{i=1}^{n} \nabla_{\lambda} \mathcal{L}(\mathcal{F}(x_i^v, \hat{\theta}_{\phi}(\lambda)), y_i^v). \tag{3}$$

Exploit-and-Explore. This step is expressed as $\lambda_i = \lambda + \epsilon_i$.

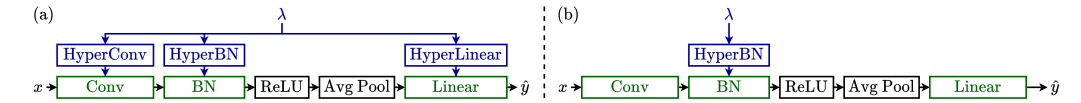


Figure 1: (a) We show an toy example network with three trainable layers (in green) and its linear hypernetwork (in blue), which consists of three linear hyper-layers. (b) If we run Algorithm 1 and share the parameters of the Conv and Linear layers, then it corresponds to running Algorithm 2 with a simplified hypernetwork, which only has a HyperBN layer.

Update. Furthermore, by substituting $\lambda_i = \lambda + \epsilon_i$ into Equation 2, we merge the Exploit-and-Explore step into the Update step and obtain

$$\phi = \phi - \alpha \frac{1}{n} \sum_{i=1}^{n} \nabla_{\phi} \mathcal{L}(\mathcal{F}(\mathcal{A}(x_i; \lambda + \epsilon_i); \hat{\theta}_{\phi}(\lambda + \epsilon_i)), y_i). \tag{4}$$

Up to now, the baseline algorithm has been modified into a gradient-based algorithm that alternates between updating ϕ (Equation 4) and λ (Equation 3). We show the modified algorithm in Algorithm 5 in Appendix B.

Main Algorithm. Lastly, instead of using the same perturbation noise $\{\epsilon_i\}_{i=1}^n$ across the T_{train} SGD steps (Equation 4), we re-sample $\{\epsilon_i\}_{i=1}^n$ for each iteration to enhance the sample diversity. In other words, at each SGD step, we sample a different discrete set of models from the hypernetwork to update its parameters. With this modification, we finally arrive at our HBA algorithm, as shown in Algorithm 2. We show the computation graph of Equation 3 and 4 in Figure 2 in Appendix F.

Algorithm 2 The main algorithm of HBA.

```
1: Input: batch size n, number of steps T_{outer}, T_{train} and T_{val}, training set D_T, augmentation
        policy A, neural network \mathcal{F}, learning rates \alpha and \alpha', validation set D_V, Gaussian sigma \sigma.
  2: Initialize \phi and \lambda
  3: for j = 1 to T_{outer} do
             for t=1 to T_{train} do

Sample \{(x_i,y_i)\}_{i=1}^n from D_T
\{\epsilon_i\}_{i=1}^n \sim N(0,\sigma)
\phi = \phi - \alpha \frac{1}{n} \sum_{i=1}^n \nabla_{\phi} \mathcal{L}(\mathcal{F}(\mathcal{A}(x_i;\lambda + \epsilon_i), \hat{\theta}_{\phi}(\lambda + \epsilon_i)), y_i)
  4:
  5:
  6:
  7:
                                                                                                                                                        \triangleright Update \phi (Equation 4)
              end for
  8:
             \begin{aligned} & \text{for } t = 1 \text{ to } T_{val} \text{ do} \\ & \text{Sample } \{(x_i^v, y_i^v)\}_{i=1}^n \text{ from } D_V \\ & \lambda = \lambda - \alpha' \frac{1}{n} \sum_{i=1}^n \nabla_{\lambda} \mathcal{L}(\mathcal{F}(x_i^v, \hat{\theta}_{\phi}(\lambda)), y_i^v) \end{aligned}
  9:
10:
                                                                                                                                                                 \triangleright Update \lambda (Equation 3)
11:
              end for
12:
13: end for
14: Output: \hat{\theta}_{\phi}(\lambda)
```

3.5 Hypernetworks

We now turn back to the design and construction of our hypernetworks mentioned in Section 3.3. Recall that a hypernetwork takes the hyperparameters λ as inputs and generates the parameters θ of a neural network. Prior work STN [9] uses a linear neural network as the hypernetwork. Unfortunately, even a linear hypernetwork requires a prohibitively large number of parameters, which would be $|\lambda||\theta|$. STN assumes that the linear transform matrix is low-rank to effectively reduce the parameter complexity from $O(|\lambda||\theta|)$ to $O(|\lambda|+|\theta|)$. Given the architecture of a neural network, its linear hypernetwork is constructed in a layer-wise manner: for each trainable layer of the neural network, we associate it with a linear hyper-layer accordingly. In Figure 1(a), we show a toy example network and its corresponding hypernetwork. In this example, since the network has three trainable layers: a convolutional (Conv) layer, a batch normalization (BN) layer, and a linear layer, we associate each of the three layers with a linear hyper-layer to construct the linear hypernetwork. We adopt the linear hyper-layers proposed by STN. Since STN lacks a hyper-layer for BN, we follow their design spirit and propose a HyperBN layer, which takes λ as input and outputs the affine parameters $\theta_{\rm BN} \in \mathbb{R}^c$ of the BN layer by $\theta_{\rm BN} = {\rm HyperBN}(\lambda; \phi_b, \phi_U, \phi_V) = \phi_b + {\rm diag}(\phi_V\lambda)\phi_U$, where $\phi_b, \phi_U \in \mathbb{R}^c$,

T-1.1. 0. A1.1.4	11.00	X7.1'.1.4'
Table 2: Abiation study on t	different weight sharing strategies.	vandation errors are reported.

		ide-ResNet-40-2	WideResNet-28-10				
Hyper-layers	Val. Error (%)	CIFAR-100 Val. Error (%)	Time (GPU Hours)	CIFAR-10 Val. Error (%)	CIFAR-100 Val. Error (%)	Time (GPU Hours)	
Conv + BN	4.01 ± 0.09	22.66 ± 0.19	2.03	2.85 ± 0.13	19.15 ± 0.21	7.74	
Conv	3.94 ± 0.08	22.71 ± 0.34	1.53	2.88 ± 0.06	19.18 ± 0.26	6.85	
BN	3.86 ± 0.08	22.86 ± 0.22	1.33	2.74 ± 0.05	19.18 ± 0.34	4.23	
1st Conv	3.85 ± 0.06	22.66 ± 0.40	0.86	2.81 ± 0.07	19.39 ± 0.25	3.36	
1st BN	4.02 ± 0.11	22.20 ± 0.10	0.87	2.72 ± 0.12	18.80 ± 0.34	3.37	

 $\phi_V \in \mathbb{R}^{c \times |\lambda|}$, and $\operatorname{diag}(\cdot)$ turns a vector into a diagonal matrix. Due to the space limit, please refer to Appendix D for the details of the hyper-layers.

Weight Sharing across Models. We propose a weight sharing strategy that can effectively reduce both the search time and the memory consumption of our method. The central idea is: adopting a weight sharing strategy in Algorithm 1 corresponds to using a simplified hypernetwork in Algorithm 2. Specifically, under the perspective of population-based training (Algorithm 1), training a set of models with weight sharing can be viewed as a multi-task training, where the i-th task corresponds to training model i with hyperparameters λ_i . If all the members of the population share a particular layer's parameters, then it equivalently means that the corresponding hyper-layer in Algorithm 2 is a constant function independent of hyperparameters. In other words, if we share a layer's parameters in Algorithm 1, there is no need to pair it with a hyper-layer in Algorithm 2. By doing so, our hypernetwork becomes smaller, and the training speed becomes faster. In Figure 1(b), we show an example of hypernetwork that corresponds to a population-based training with weight sharing applied to the Conv and Linear layers.

4 Experiments

We first present an ablation study of weight sharing strategies and then evaluate our HBA on four image classification datasets: CIFAR-10 [13], CIFAR-100 [13], SVHN [15], and ImageNet [16]. We compare HBA with standard augmentation (Baseline), Cutout [20], AutoAugment (AA) [1], Population Based Augmentation (PBA) [2], Fast AutoAugment (FAA) [3], OHL-Auto-Aug (OHLAA) [26], RandAugment (RA) [27], Adversarial AutoAugment (AdvAA) [32], and Differentiable Automatic Data Augmentation (DADA) [28]. Lastly, we compare with Self-Tuning Network (STN) [9] on hyperparameter optimization.

Implementation Details. Following PBA [2], our search space consists of 15 operations, where each has two copies. Please see Appendix A for the list of operations and their hyperparameters. Following STN [9], HBA trained the hypernetwork parameters using SGD with $T_{train}=2$ and optimized the hyperparameters using Adam [33] with $T_{val}=1$. We implemented HBA using the Pytorch [34] framework. We measured the search time of HBA on an NVIDIA Tesla V100 GPU. We reported the performance of the last epoch after training for all of our results using the mean and standard deviation over five runs with different random seeds. For policy evaluation, we scaled the length of the discovered schedules linearly if necessary.

4.1 Ablation Study

We conducted an ablation study on different weight sharing strategies. In general, if we share a subset of the trainable layers' parameters from the perspective of population-based training, it means that we do not associate them with hyper-layers. We experimented with five weight sharing strategies: Conv+BN, Conv, BN, 1st Conv, and 1st BN. These strategies are named by what layers are added with hyper-layers. For example, the second strategy (Conv) means that we add HyperConv layers to all the convolutional layers and ignore the other layers. All strategies did not add a hyper-layer to the last linear layer of the network, which performed better in our preliminary experiments. The intuition behind such strategies is as follows. For the low-level layers, we do not share parameters so that they are enforced to reflect the influence of different augmentation policies. For the mid and highlevel layers, we share parameters to encourage the population to learn a joint feature representation. In this study, we split the CIFAR training set into three sets (30k/10k/10k) and denoted them as Train30k/Val0/Val. The CIFAR test set was not used. For *policy search*, we applied HBA to train on the Train30k/Val0 split to find policies. For *policy evaluation*, we used the searched policies to train networks on the Train30k+Val0 set and evaluated them on the Val set. Table 2 shows the comparison

Table 3: Comparison of search time in GPU hours.

	AA	PBA	FAA	OHLAA	AdvAA	DADA	HBA
GPU	P100	Titan XP	V100	-	V100	Titan XP	V100
CIFAR-10	5000	5	3.5	83.4	-	0.1	0.1
SVHN	1000	1	1.5	-	-	0.1	0.1
ImageNet	15000	-	450	625	1280	1.3	0.9

Table 4: CIFAR-10 and CIFAR-100 test error rates (%). WRN, SS, and PN+SD are the shorthand of Wide-ResNet, Shake-Shake, and PyramidNet+ShakeDrop, respectively.

	Baseline	Cutout	AA	PBA	FAA	RA	AdvAA	DADA	HBA
CIFAR-10									
WRN-40-2	5.3	4.1	3.7	-	3.6	-	-	3.6	3.80 ± 0.15
WRN-28-10	3.9	3.1	2.6	2.6	2.7	2.7	1.9	2.7	2.63 ± 0.10
SS (26 2x32d)	3.6	3.0	2.5	2.5	2.7	-	2.4	2.7	2.63 ± 0.16
SS (26 2x96d)	2.9	2.6	2.0	2.0	2.0	2.0	1.9	2.0	2.03 ± 0.10
SS (26 2x112d)	2.8	2.6	1.9	2.0	2.0	-	1.8	2.0	1.97 ± 0.05
PN+SD	2.7	2.3	1.5	1.5	1.8	1.7	1.4	1.7	1.58 ± 0.06
CIFAR-100									
WRN-40-2	26.0	25.2	20.7	-	20.7	-	-	20.9	20.60 ± 0.37
WRN-28-10	18.8	18.4	17.1	16.7	17.3	16.7	15.5	17.5	17.46 ± 0.48
SS (26 2x96d)	17.1	16.0	14.3	15.3	14.9	-	14.1	15.3	15.35 ± 0.38
PN+SD	14.0	12.2	10.7	10.9	11.9	-	10.4	11.2	12.10 ± 0.14

results between these five strategies. We can see that adding fewer hyper-layers reduces search time and achieves slightly better performance across different datasets and models. Based on the ablation results, we employ the 1st BN strategy in the subsequent experiments.

4.2 Main Results

Settings. For each dataset, we randomly sampled a subset of 10,000 images from the original training set as the validation set D_V for HBA. Following the experimental setting of [1, 2, 3], we randomly sampled a subset from the remaining images to create a reduced version of the training set. For *policy search*, we applied HBA to train a Wide-ResNet-40-2 (WRN-40-2) [14] network on the reduced datasets. For *policy evaluation*, we evaluated the performance of a model M by using the searched policy to train M on the original training set and measuring the accuracy on the test set. Please see Table 10 and 11 in Appendix E for the detailed hyperparameter settings.

CIFAR-10 and CIFAR-100. The CIFAR-10 and CIFAR-100 datasets consist of 60,000 natural images, with a size of 32x32. The training and test sets have 50,000 and 10,000 images, respectively. We applied our augmentation policy, baseline, and Cutout (with 16x16 pixels) in sequence to each training image. The baseline augmentation is defined as the following operations in sequence: standardization, horizontal flipping, and random cropping. We evaluated our searched policies with Wide-ResNet-40-2 (WRN-40-2) [14], Wide-ResNet-28-10 (WRN-28-10) [14], Shake-Shake [35], and PyramidNet+ShakeDrop [36]. As shown in Table 3 and 4, HBA significantly improves the performance over the baseline and Cutout, while achieving competitive accuracy with the compared methods. HBA only takes 0.2 GPU hours on the Reduced CIFAR-10 for policy search, which is an order of magnitude faster than PBA (population-based method) and is comparable to DADA (gradient-based method).

SVHN. The SVHN dataset consists of 73,257 training images (called core training set), 531,131 additional training images, and 26,032 test images. We applied our augmentation policy, baseline, and Cutout (with 20x20 pixels) in sequence to each training image. The baseline augmentation applied standardization only. We evaluated our searched policies with WRN-40-2, WRN-28-10, and Shake-Shake. As shown in Table 3 and 5, HBA achieves competitive accuracy and slightly outperforms PBA and DADA.

ImageNet. The ImageNet dataset has a training set of about 1.2M images and a validation set of 50,000 images. We applied our augmentation policy and then the baseline augmentation to each training image. Following [3], the baseline augmentation applied random resized crop, horizontal flip, color jittering, PCA jittering, and standardization in sequence. We evaluated our searched policies

Table 5: SVHN test error rates (%).

Model	Baseline	Cutout	AA	PBA	FAA	RA	DADA	HBA
Wide-ResNet-28-10 Shake-Shake (26 2x96d)								

Table 6: ImageNet validation error rates of ResNet-50.

	Baseline	AA	FAA	OHLAA	RA	AdvAA	DADA	HBA
Top-1 Error (%) Top-5 Error (%)								

Table 7: Comparison between policy search on a proxy task (top half) and target tasks (bottom half).

P	olicy Search		Policy Evaluation			
Dataset	Model	Time (GPU hours)	Dataset	Model	Test Error (%)	
Reduced CIFAR-10	WRN-40-2	0.1	CIFAR-10 CIFAR-100 CIFAR-10 CIFAR-100	WRN-40-2 WRN-28-10	3.78 ± 0.15 20.58 ± 0.37 2.63 ± 0.10 17.46 ± 0.48	
CIFAR-10 CIFAR-100	WRN-40-2	1.2 ↑	CIFAR-10 CIFAR-100	WRN-40-2	$3.63 \pm 0.07 \downarrow 20.80 \pm 0.28 \uparrow$	
CIFAR-10 CIFAR-100	WRN-28-10	4.5 ↑	CIFAR-10 CIFAR-100	WRN-28-10	$2.59 \pm 0.09 \downarrow \\ 16.87 \pm 0.22 \downarrow$	

Table 8: Comparison with STN [9] on CIFAR-10 using AlexNet.

	Validation Loss	Test Loss	Test Error (%)
STN	$\begin{array}{c} 0.579 \pm 0.005 \\ 0.548 \pm 0.005 \end{array}$	0.582 ± 0.004	19.86 ± 0.21
HBA		0.556 ± 0.005	18.76 ± 0.11

with ResNet-50 [17]. As shown in Table 3 and 6, HBA is at least three orders of magnitude faster than all the compared methods except DADA. Compared with DADA, HBA achieves higher accuracy.

Policy Search on the Target Tasks. In the previous experiments (Table 3, 4, 5, 6), we applied HBA on a *reduced* task, which trains a smaller network (WRN-40-2) on a reduced dataset. Here, We compared with the performance of policy searched on the *target* tasks, which trains the target network on the full dataset to find the augmentation policy. We consider training a model $M \in \{\text{WRN-40-2}, \text{WRN-28-10}\}$ on a dataset $D \in \{\text{CIFAR-10}, \text{CIFAR-100}\}$, giving us four target tasks. Table 7 shows that training on target tasks requires longer search time while achieving slightly better performances (in three out of four cases), which is similar to the findings in RA [27] and DADA [28].

4.3 Comparison with STN

We followed the experiment settings of STN [9] and applied HBA to simultaneously train an AlexNet [19] model and tune the regularization hyperparameters on CIFAR-10. We employed the Conv strategy to construct our hypernetwork for the AlexNet model. As shown in Table 8, HBA performs much better than STN, showing the effectiveness of our weight sharing strategy.

5 Conclusion

In this paper, we proposed Hypernetwork-Based Augmentation (HBA) for automated data augmentation. HBA employs a hypernetwork to train a continuous set of models and uses gradient descent to tune augmentation hyperparameters. Our weight sharing strategy improved both the search speed and accuracy. Experimental results showed that HBA is significantly faster than the state-of-the-art methods while offering comparable accuracy. Future directions include: (1) applying HBA to medical image datasets, (2) exploring hybrid algorithms that interpolates between PBT and HBA, and (3) determining the hypernetwork architecture by neural architecture search methods.

6 Broader Impact

Our work is a new algorithm for automated data augmentation, which can be treated as a specific technical component in an AutoML system. On the one hand, AutoML makes it easier for non-experts to make use of machine learning models and techniques. On the other hand, AutoML helps machine learning researchers to lift the focus of development from feature design to architecture design and optimization scheme design.

References

- [1] Ekin D Cubuk, Barret Zoph, Dandelion Mane, Vijay Vasudevan, and Quoc V Le. AutoAugment: Learning augmentation strategies from data. In *CVPR*, 2019.
- [2] Daniel Ho, Eric Liang, Ion Stoica, Pieter Abbeel, and Xi Chen. Population based augmentation: Efficient learning of augmentation policy schedules. In *ICML*, 2019.
- [3] Sungbin Lim, Ildoo Kim, Taesup Kim, Chiheon Kim, and Sungwoong Kim. Fast AutoAugment. In NeurIPS, 2019.
- [4] Qizhe Xie, Zihang Dai, Eduard Hovy, Minh-Thang Luong, and Quoc V Le. Unsupervised data augmentation. *arXiv preprint arXiv:1904.12848*, 2019.
- [5] David Berthelot, Nicholas Carlini, Ian Goodfellow, Nicolas Papernot, Avital Oliver, and Colin A Raffel. MixMatch: A holistic approach to semi-supervised learning. In *Advances in Neural Information Processing Systems*, pages 5050–5060, 2019.
- [6] Ting Chen, Simon Kornblith, Mohammad Norouzi, and Geoffrey Hinton. A simple framework for contrastive learning of visual representations. *arXiv preprint arXiv:2002.05709*, 2020.
- [7] Ilya Kostrikov, Denis Yarats, and Rob Fergus. Image augmentation is all you need: Regularizing deep reinforcement learning from pixels. *arXiv preprint arXiv:2004.13649*, 2020.
- [8] Sergey Ioffe and Christian Szegedy. Batch normalization: Accelerating deep network training by reducing internal covariate shift. In *ICML*, 2015.
- [9] Matthew MacKay, Paul Vicol, Jon Lorraine, David Duvenaud, and Roger Grosse. Self-tuning networks: Bilevel optimization of hyperparameters using structured best-response functions. In *ICLR*, 2019.
- [10] Hieu Pham, Melody Y Guan, Barret Zoph, Quoc V Le, and Jeff Dean. Efficient neural architecture search via parameter sharing. *arXiv preprint arXiv:1802.03268*, 2018.
- [11] Andrew Brock, Theodore Lim, James M Ritchie, and Nick Weston. SMASH: one-shot model architecture search through hypernetworks. In *ICLR*, 2018.
- [12] Gabriel Bender, Pieter-Jan Kindermans, Barret Zoph, Vijay Vasudevan, and Quoc Le. Understanding and simplifying one-shot architecture search. In *ICML*, 2018.
- [13] Alex Krizhevsky and Geoffrey Hinton. Learning multiple layers of features from tiny images. *Technical Report*, 2009.
- [14] Sergey Zagoruyko and Nikos Komodakis. Wide residual networks. In BMVC, 2016.
- [15] Yuval Netzer, Tao Wang, Adam Coates, Alessandro Bissacco, Bo Wu, and Andrew Y. Ng. Reading digits in natural images with unsupervised feature learning. In NIPS Workshop on Deep Learning and Unsupervised Feature Learning 2011, 2011.
- [16] Jia Deng, Wei Dong, Richard Socher, Li-Jia Li, Kai Li, and Li Fei-Fei. ImageNet: A large-scale hierarchical image database. In *CVPR*, 2009.
- [17] Kaiming He, Xiangyu Zhang, Shaoqing Ren, and Jian Sun. Deep residual learning for image recognition. In CVPR, 2016.
- [18] Connor Shorten and Taghi M Khoshgoftaar. A survey on image data augmentation for deep learning. *Journal of Big Data*, 2019.
- [19] Alex Krizhevsky, Ilya Sutskever, and Geoffrey E Hinton. Imagenet classification with deep convolutional neural networks. In *Advances in neural information processing systems*, 2012.
- [20] Terrance DeVries and Graham W Taylor. Improved regularization of convolutional neural networks with cutout. *arXiv preprint arXiv:1708.04552*, 2017.
- [21] Hongyi Zhang, Moustapha Cisse, Yann N Dauphin, and David Lopez-Paz. mixup: Beyond empirical risk minimization. In *ICLR*, 2018.

- [22] Sangdoo Yun, Dongyoon Han, Seong Joon Oh, Sanghyuk Chun, Junsuk Choe, and Youngjoon Yoo. CutMix: Regularization strategy to train strong classifiers with localizable features. In ICCV, 2019.
- [23] Barret Zoph and Quoc V Le. Neural architecture search with reinforcement learning. In ICLR, 2017.
- [24] Hanxiao Liu, Karen Simonyan, and Yiming Yang. DARTS: Differentiable architecture search. In *ICLR*, 2019.
- [25] Max Jaderberg, Valentin Dalibard, Simon Osindero, Wojciech M Czarnecki, Jeff Donahue, Ali Razavi, Oriol Vinyals, Tim Green, Iain Dunning, Karen Simonyan, et al. Population based training of neural networks. *arXiv preprint arXiv:1711.09846*, 2017.
- [26] Chen Lin, Minghao Guo, Chuming Li, Xin Yuan, Wei Wu, Junjie Yan, Dahua Lin, and Wanli Ouyang. Online hyper-parameter learning for auto-augmentation strategy. In *ICCV*, 2019.
- [27] Ekin D Cubuk, Barret Zoph, Jonathon Shlens, and Quoc V Le. RandAugment: Practical automated data augmentation with a reduced search space. arXiv preprint arXiv:1909.13719, 2019.
- [28] Yonggang Li, Guosheng Hu, Yongtao Wang, Timothy Hospedales, Neil M Robertson, and Yongxing Yang. DADA: Differentiable automatic data augmentation. *arXiv* preprint *arXiv*:2003.03780, 2020.
- [29] David Ha, Andrew Dai, and Quoc V Le. Hypernetworks. In *ICLR*, 2017.
- [30] Tong Yu and Hong Zhu. Hyper-parameter optimization: A review of algorithms and applications. *arXiv preprint arXiv:2003.05689*, 2020.
- [31] Nitish Srivastava, Geoffrey Hinton, Alex Krizhevsky, Ilya Sutskever, and Ruslan Salakhutdinov. Dropout: a simple way to prevent neural networks from overfitting. *JMLR*, 2014.
- [32] Xinyu Zhang, Qiang Wang, Jian Zhang, and Zhao Zhong. Adversarial AutoAugment. In ICLR, 2020.
- [33] Diederick P Kingma and Jimmy Ba. Adam: A method for stochastic optimization. In ICLR, 2015.
- [34] Adam Paszke, Sam Gross, Francisco Massa, Adam Lerer, James Bradbury, Gregory Chanan, Trevor Killeen, Zeming Lin, Natalia Gimelshein, Luca Antiga, et al. PyTorch: An imperative style, high-performance deep learning library. In *Advances in Neural Information Processing Systems*, 2019.
- [35] Xavier Gastaldi. Shake-shake regularization. In ICLR, 2017.
- [36] Yoshihiro Yamada, Masakazu Iwamura, Takuya Akiba, and Koichi Kise. Shakedrop regularization for deep residual learning. *IEEE Access*, 2019.

Appendix A Search space

Elementary Image Operations. Table 9 shows the list of augmentation operations used in our search space. When applying an operation $op \in \{\text{ShearX}, \text{ShearY}, \text{TranslateX}, \text{TranslateY}, \text{Rotate}\}$ to an input image, we randomly negate the sampled magnitude with a probability of 0.5.

Augmentation Function. Our search space is based on PBA [2]. Please refer to the Algorithm 1 in the PBA paper for the augmentation function used for both PBA and our HBA.

Initialization. For each augmentation hyperparameter, we initialize its value by $0.95M_{\min} + 0.05M_{\max}$, where $[M_{\min}, M_{\max}]$ is the magnitude range of the hyperparameter.

Implementation Details. Following STN [9], we define the hyperparameters λ as the unbounded version of the operation magnitudes and probabilities by mapping a range of magnitude $[M_{\min}, M_{\max}]$ to $[-\infty, \infty]$ through a logit function (the inverse of the sigmoid function). The magnitude range of each operation is shown in Table 9, and the probability range of each operation is [0, 1].

Table 9: List of augmentation operations.

Tuble 9. Elst of augmentation operations.						
Operation	Range of Magnitude	Unit of Magnitude				
ShearX	[0, 0.3]	-				
ShearY	[0, 0.3]	-				
TranslateX	[0, 0.45]	Image size				
TranslateY	[0, 0.45]	Image size				
Rotate	[0, 30]	Degree				
AutoContrast	None	=				
Invert	None	-				
Equalize	None	-				
Solarize	[0, 255]	-				
Posterize	[0, 8]	Bit				
Contrast	[0.1, 1.9]	-				
Color	[0.1, 1.9]	-				
Brightness	[0.1, 1.9]	-				
Sharpness	[0.1, 1.9]	-				
Cutout	[0, 0.2]	Image size				

Appendix B The Derivation of Hypernetwork-Based Augmentation (HBA)

Algorithm 3, 4, 5, and 6 show the derivation of our algorithm from a population-based to a gradient-based training algorithm. For each algorithm, we highlight the changes from the previous algorithm in blue. The high-level description of these four algorithms are:

- Algorithm 3: training a population of models by stochastic gradient descent.
- Algorithm 4: representing a population of models by a hypernetwork.
- Algorithm 5: approximating model selection by stochastic gradient descent.
- Algorithm 6: the main algorithm.

Algorithm 3 The baseline algorithm of HBA Algorithm 4 The modified baseline algorithm in Section 3.2. in Section 3.3. 1: **Input:** population size n, number of steps T_{outer} 1: **Input:** batch size n, number of steps T_{outer} and and T_{train} , training set D_T , augmentation policy T_{train} , training set D_T , augmentation policy \mathcal{A} , A, neural network F, learning rate α , validation set neural network \mathcal{F} , learning rate α , validation set D_V , Gaussian sigma σ and σ' . D_V , Gaussian sigma σ . 2: Initialize $\{\theta_i\}_{i=1}^n$ and $\{\lambda_i\}_{i=1}^n$ 2: Initialize ϕ and $\{\lambda_i\}_{i=1}^n$ 3: for j = 1 to T_{outer} do 3: for j = 1 to T_{outer} do for i=1 to n (synchronously in parallel) do 4: for t=1 to T_{train} do 5: 5: for t=1 to T_{train} do Sample $\{(x, y)\}_{i=1}^n$ from D_T $\phi = \phi - \alpha \frac{1}{n} \sum_{i=1}^n \nabla_{\phi}$ 6: Sample (x, y) from D_T 6: 7: $\theta_i = \theta_i - \alpha \nabla_{\theta} \mathcal{L}(\mathcal{F}(\mathcal{A}(x; \lambda_i); \theta_i), y)$ 7: $\mathcal{L}(\mathcal{F}(\mathcal{A}(x_i;\lambda_i),\hat{\theta}_{\phi}(\lambda_i)),y_i)$ 8: end for 8: 9: end for 9: $k = \underset{\sum_{(x^v, y^v) \in D_V}}{\arg\min_{i \in \{1, \dots, n\}}} \mathcal{L}(\mathcal{F}(x^v; \theta_i), y^v)$ 10: 10: $k = \arg\min_{i \in \{1, \dots, n\}}$ $\sum_{(x^v, y^v) \in D_V} \mathcal{L}(\mathcal{F}(x^v; \hat{\theta}_{\phi}(\lambda_i)), y^v)$ for i = 1 to n do for i = 1 to n do 11: 11: 12: $\lambda_i = \lambda_k + \epsilon_i$ where $\epsilon_i \sim N(0, \sigma)$ 12: $\lambda_i = \lambda_k + \epsilon_i \text{ where } \epsilon_i \sim N(0, \sigma)$ $\theta_i = \theta_k + \epsilon_i'$ where $\epsilon_i' \sim N(0, \sigma')$ 13: end for 13: 14: end for 14: 15: end for 15: end for 16: Output: $\hat{\theta}_{\phi}(\lambda_k)$ 16: Output: θ_k

Algorithm 5 The modified baseline algorithm in Section 3.4.

Algorithm 6 The main algorithm of HBA in Section 3.4.

```
1: Input: batch size n, number of steps T_{outer}, T_{train}, 1: Input: batch size n, number of steps T_{outer}, T_{train},
      and T_{val}, training set D_T, augmentation policy A,
                                                                                                     and T_{val}, training set D_T, augmentation policy \mathcal{A},
      neural network \mathcal{F}, learning rate \alpha and \alpha', validation
                                                                                                     neural network \mathcal{F}, learning rate \alpha and \alpha', validation
      set D_V, Gaussian sigma \sigma.
                                                                                                     set D_V, Gaussian sigma \sigma.
 2: Initialize \phi and \lambda
                                                                                                2: Initialize \phi and \lambda
 3: for j = 1 to T_{outer} do
                                                                                                3: for j = 1 to T_{outer} do
                                                                                                4:
                                                                                                         for t=1 to T_{train} do
 4:
           \{\epsilon_i\}_{i=1}^n \sim N(0,\sigma)
           for t = 1 to T_{train} do
 5:
                                                                                                5:
                                                                                                              Sample \{(x,y)\}_{i=1}^n from D_T
                Sample \{(x,y)\}_{i=1}^n from D_T

\phi = \phi - \alpha \frac{1}{n} \sum_{i=1}^n \nabla_{\phi}
                                                                                                              \begin{cases} \epsilon_i \end{cases}_{i=1}^n \sim N(0, \sigma) \\ \phi = \phi - \alpha \frac{1}{n} \sum_{i=1}^n \nabla_{\phi} \end{cases}
 6:
                                                                                                6:
 7:
                                                                                                7:
                         \mathcal{L}(\mathcal{F}(\mathcal{A}(x_i; \lambda + \epsilon_i), \hat{\theta}_{\phi}(\lambda + \epsilon_i)), y_i)
                                                                                                                       \mathcal{L}(\mathcal{F}(\mathcal{A}(x_i; \lambda + \epsilon_i), \hat{\theta}_{\phi}(\lambda + \epsilon_i)), y_i)
 8:
           end for
                                                                                                8:
                                                                                                         end for
           for t=1 to T_{val} do
                                                                                                         for t=1 to T_{val} do
 9:
                                                                                               9:
                Sample \{(x_i^v, y_i^v)\}_{i=1}^n from D_V
                                                                                                              Sample \{(x_i^v, y_i^v)\}_{i=1}^n from D_V
10:
                                                                                              10:
                                                                                                              \lambda = \lambda - \alpha' \frac{1}{n} \sum_{i=1}^{n} \nabla_{\lambda} \mathcal{L}(\mathcal{F}(x_{i}^{v}, \hat{\theta}_{\phi}(\lambda)), y_{i}^{v})
                \lambda = \lambda - \alpha' \frac{1}{n} \sum_{i=1}^{n} \nabla_{\lambda} \mathcal{L}(\mathcal{F}(x_i^v, \hat{\theta}_{\phi}(\lambda)), y_i^v) 11:
11:
12:
            end for
                                                                                                          end for
13: end for
                                                                                              13: end for
14: Output: \hat{\theta}_{\phi}(\lambda)
                                                                                              14: Output: \hat{\theta}_{\phi}(\lambda)
```

Appendix C Our Baseline Algorithm is a Special Case of PBT

Our baseline algorithm (Algorithm 3) can be expressed in the format of PBT [25] as follows:

Step: each model runs an SGD step with a batch size of 1.

Eval: we evaluate each model on a validation set by cross entropy loss.

Ready: each model goes through the exploit-and-explore process every T_{train} steps.

Exploit: each model clones the weights and hyperparameters of the best performing model.

Explore: for each model, we perturb the value of its parameters and hyperparameters.

Algorithm 7 The baseline algorithm of HBA in the format of PBT.

```
1: Input: population size n, number of steps T_{outer} and T_{train}, training set D_T, augmentation policy \mathcal{A},
     neural network \mathcal{F}, learning rate \alpha, validation set D_V, Gaussian sigma \sigma and \sigma'.
 2: Initialize \{\theta_i\}_{i=1}^n and \{\lambda_i\}_{i=1}^n
 3: for j = 1 to T_{outer} do
         for i = 1 to n (synchronously in parallel) do
             for t=1 to T_{train} do
 5:
 6:
                 // Step
 7:
                 Sample (x, y) from D_T
 8:
                 \theta_i = \theta_i - \alpha \nabla_{\theta} \mathcal{L}(\mathcal{F}(\mathcal{A}(x; \lambda_i); \theta_i), y)
 9:
             end for
10:
         end for
11:
         // Eval
         k = \arg\min_{i \in \{1,\dots,n\}} \sum_{(x^v, y^v) \in D_V} \mathcal{L}(\mathcal{F}(x^v; \theta_i), y^v)
12:
13:
         // Exploit
14:
         for i=1 to n do
15:
             \lambda_i = \lambda_k
             \theta_i = \theta_k
16:
17:
         end for
18:
         // Explore
19:
         for i = 1 to n do
20:
              \lambda_i = \lambda_i + \epsilon_i where \epsilon_i \sim N(0, \sigma)
21:
             \theta_i = \theta_i + \epsilon_i' where \epsilon_i' \sim N(0, \sigma')
22:
         end for
23: end for
24: Output: \theta_k
```

Appendix D Hyper-layers

HyperLinear Layer. Let f be a linear layer. We have

$$y = f(x; W) = Wx, (5)$$

where $x \in \mathbb{R}^{c_1}$, $y \in \mathbb{R}^{c_2}$, and the weight matrix $W \in \mathbb{R}^{c_2 \times c_1}$ is the parameters of the linear layer.

Given a linear layer f, we define its corresponding HyperLinear layer \hat{W} as a linear function that maps hyperparameters $\lambda \in \mathbb{R}^n$ to the weight matrix $W \in \mathbb{R}^{c_2 \times c_1}$ of the linear layer f. We can decompose the hyperlinear layer \hat{W} into a set linear functions $\{\hat{w}_i(\lambda)\}_{i=1}^{c_2}$ that each function $\hat{w}_i(\lambda)$ outputs the transpose of the i-th row of W. \hat{W} can be expressed as

$$W = \hat{W}(\lambda) = [\hat{w}_1(\lambda), ..., \hat{w}_{c_2}(\lambda)]^T$$
(6)

and
$$\hat{w}_i(\lambda) = w_i + A_i \lambda,$$
 (7)

where $A_i \in \mathbb{R}^{c_1 \times n}$ and $w_i \in \mathbb{R}^{c_1}$. A HyperLinear layer parameterized by $\{A_i\}_{i=1}^{c_2}$ and $\{w_i\}_{i=1}^{c_2}$ requires nc_1c_2 and c_1c_2 parameters, respectively. Due to its prohibitively huge memory consumption, following Self-Tuning Network (STN) [9], we assume A_i is a rank-1 matrix to greatly reduce the number of parameters of the HyperLinear layer. Specifically, we define $A_i = u_i v_i^T$ where $u_i \in \mathbb{R}^{c_1}$ and $v_i \in \mathbb{R}^n$. By doing so, the number of parameters of the HyperLinear layer is reduced to $(n+c_1)c_2+c_1c_2$. $\hat{w}_i(\lambda)$ is written as

$$\hat{w}_i(\lambda) = w_i + A_i \lambda = w_i + u_i v_i^T \lambda = w_i + (v_i^T \lambda) u_i.$$
(8)

The HyperLinear layer $\hat{W}(\lambda)$ can then be expressed as

$$W = \hat{W}(\lambda) = [\hat{w}_1(\lambda), ..., \hat{w}_{c_2}(\lambda)]^T = W_0 + \operatorname{diag}(V\lambda)U$$
(9)

where $W_0 = [w_1,...,w_{c_2}]^T \in \mathbb{R}^{c_2 \times c_1}$, $V = [v_1,...,v_{c_2}]^T \in \mathbb{R}^{c_2 \times n}$, $U = [u_1,...,u_{c_2}]^T \in \mathbb{R}^{c_2 \times c_1}$, and $\operatorname{diag}(\cdot)$ turns a vector into a diagonal matrix. In particular, W,W_0 , and U have the same matrix size.

Let W_0 , U, and V be denoted by ϕ_0 , ϕ_U , and ϕ_V , respectively. The HyperLinear layer can be expressed in a general form as

$$W = \hat{W}(\lambda; \phi_0, \phi_U, \phi_V) = \phi_0 + \operatorname{diag}(\phi_V \lambda)\phi_U. \tag{10}$$

Consider a linear layer with a bias b, the bias part of the hyperLinear layer can be additionally defined in a similar way as

$$b = \hat{b}(\lambda; \phi_0^{\mathsf{b}}, \phi_U^{\mathsf{b}}, \phi_V^{\mathsf{b}}) = \phi_0^{\mathsf{b}} + \operatorname{diag}(\phi_V^{\mathsf{b}}\lambda)\phi_U^{\mathsf{b}}$$

$$\tag{11}$$

where $\phi_0^{\mathrm{b}} \in \mathbb{R}^{c_2}$, $\phi_V^{\mathrm{b}} \in \mathbb{R}^{c_2 \times n}$, and $\phi_U^{\mathrm{b}} \in \mathbb{R}^{c_2}$.

HyperConv Layer. A linear layer can be interpreted as a 1×1 convolutional layer by (1) viewing the input vector x as an image with c_1 channels and a spatial size of 1×1 , and (2) viewing the weight matrix W as the set of 1×1 convolutional filters, where each row of W is a filter. Therefore, we can define the hyper-layer of a 1×1 convolutional layer in the same way as the HyperLinear layer. We follow the definition of the HyperLinear layer (Equation 10), and define the HyperConv1x1 layer as

$$\theta_{\text{conv1x1}} = \hat{\theta}_{\text{conv1x1}}(\lambda; \phi_0^{\text{c}}, \phi_U^{\text{c}}, \phi_V^{\text{c}}) = \phi_0^{\text{c}} + \text{diag}(\phi_V^{\text{c}}\lambda)\phi_U^{\text{c}}, \tag{12}$$

where $\theta_{\text{conv1x1}}, \phi_0^{\text{c}}, \phi_U^{\text{c}} \in \mathbb{R}^{c_2 \times c_1}$ are three sets of 1×1 filters. c_1 and c_2 are the number of the input and output channels, respectively. $\operatorname{diag}(\phi_V^{\text{c}}\lambda)\phi_U^{\text{c}}$ can be interpreted as a filter-wise scaling of ϕ_U^{c} , in which the j-th filter weights of ϕ_U^{c} are scaled by the j-th element of $\phi_V^{\text{c}}\lambda$. In general, the HyperConv layer for a $k \times k$ convolutional layer can be defined with the HyperConv1x1 layer by changing ϕ_0^{c} and ϕ_U^{c} from 1×1 to $k \times k$ filters as follows:

$$\theta_{\text{conv}} = \hat{\theta}_{\text{conv}}(\lambda; \phi_0^{\text{c}}, \phi_U^{\text{c}}, \phi_V^{\text{c}}) = \phi_0^{\text{c}} + \text{diag}(\phi_V^{\text{c}}\lambda)\phi_U^{\text{c}}, \tag{13}$$

where each row of ϕ_0^c and ϕ_U^c corresponds to the parameters of a $k \times k$ filter. Specifically, $\theta_{\text{conv}}, \phi_0^c, \phi_U^c \in \mathbb{R}^{c_2 \times c_1 k^2}, \, \phi_V^c \in \mathbb{R}^{c_2 \times n}$. For a Conv layer with a bias, the bias part of the HyperConv layer is the same as the HyperLinear one (Equation 11).

HyperBN Layer. A batch normalization layer has a trainable affine transformation. Following the design spirit of the HyperLinear and the HyperConv layer, we denote the affine parameters by $\theta_{\rm BN}$ and define the HyperBN layer as

$$\theta_{\rm BN} = \text{HyperBN}(\lambda; \phi_0^{\rm BN}, \phi_U^{\rm BN}, \phi_V^{\rm BN}) = \phi_0^{\rm BN} + \text{diag}(\phi_V^{\rm BN}\lambda)\phi_U^{\rm BN}, \tag{14}$$

where $\phi_0^{\text{BN}} \in \mathbb{R}^{2c_2}$, $\phi_V^{\text{BN}} \in \mathbb{R}^{2c_2 \times n}$, $\phi_U^{\text{BN}} \in \mathbb{R}^{2c_2}$, and c_2 is the number of the output channels. There is a factor 2 because the affine transformation has c_2 scaling parameters and c_2 offset parameters.

Appendix E Hyperparameters

Table 10 and 11 show the hyperparameters used in policy search and policy evaluation, respectively. For the ImageNet dataset, we used a step-decay learning rate schedule that drops by 0.1 at epoch 90, 180, and 240.

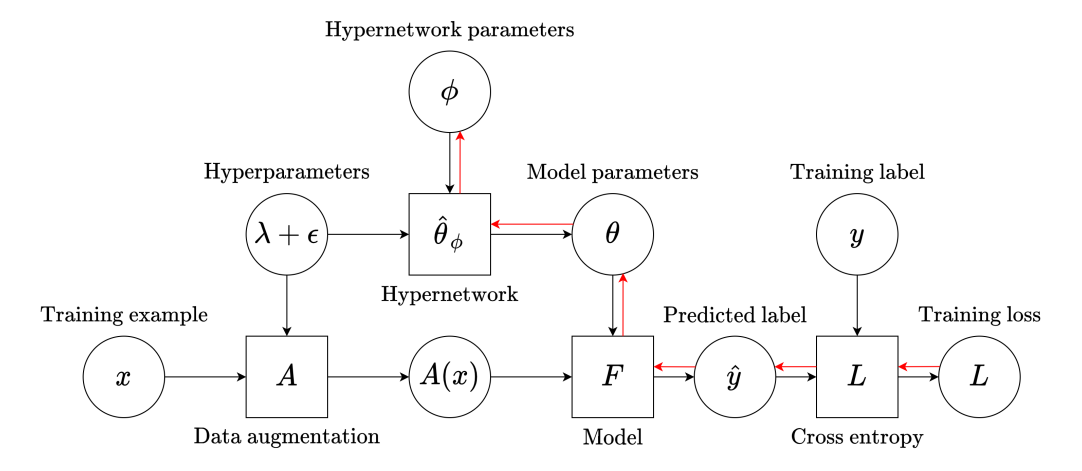
Table 10: Hyperparameters for policy search.

	71 1		1 /	
Dataset	Reduced CIFAR-10	Reduced SVHN	Reduced ImageNet	CIFAR-10 / CIFAR-100
No. classes	10	10	120	10
No. training images	4,000	4,000	6,000	40,000
No. validation images	10,000	10,000	10,000	10,000
Model	WRN-40-2	WRN-40-2	WRN-40-2	WRN-40-2 / WRN-28-10
Input size	32x32	32x32	32x32	32x32
No. training epoch	200	160	270	200
Learning rate α	0.05	0.01	0.1	0.1
Learning rate schedule (α)	cosine	cosine	step	cosine
Weight decay	0.005	0.01	0.001	0.0005
Batch size	128	128	128	128
Learning rate α'	0.03	0.02	0.007	0.003
Learning rate schedule (α')	constant	constant	constant	constant
Results in the main paper	Table 4	Table 5	Table 6	Table 7

Table 11: Hyperparameters for policy evaluation. LR: learning rate. Schedule: learning rate schedule. WD: weight decay. BS: batch size. Epoch: number of training epoch. All the hyperparameters follow the settings in PBA [2] except the ones for the ImageNet dataset. We used 8 NVIDIA Tesla V100 GPUs to train ResNet-50 on the ImageNet dataset.

Dataset	Model	LR	Schedule	WD	BS	Epoch
CIFAR-10	WRN-40-2	0.1	cosine	0.0005	128	200
CIFAR-10	WRN-28-10	0.1	cosine	0.0005	128	200
CIFAR-10	Shake-Shake (26 2x32d)	0.01	cosine	0.001	128	1800
CIFAR-10	Shake-Shake (26 2x96d)	0.01	cosine	0.001	128	1800
CIFAR-10	Shake-Shake (26 2x112d)	0.01	cosine	0.001	128	1800
CIFAR-10	PyramidNet+ShakeDrop	0.05	cosine	0.00005	64	1800
CIFAR-100	WRN-28-10	0.1	cosine	0.0005	128	200
CIFAR-100	Shake-Shake (26 2x96d)	0.01	cosine	0.0025	128	1800
CIFAR-100	PyramidNet+ShakeDrop	0.025	cosine	0.0005	64	1800
SVHN	WRN-28-10	0.005	cosine	0.001	128	160
SVHN	Shake-Shake (26 2x96d)	0.01	cosine	0.00015	128	160
ImageNet	ResNet-50	0.1	step	0.0001	256	270

Appendix F Computation graph of HBA



(a) Update hypernetwork parameters

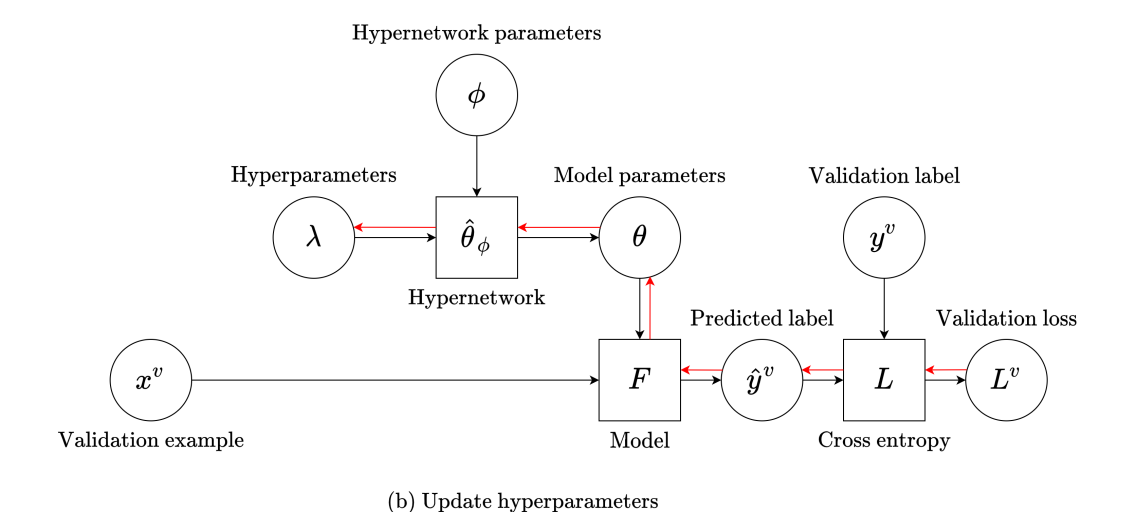


Figure 2: The computation graphs of our algorithm. The arrows in red represents the gradient flow of the backward propagation.

Preprint. Under review.